Journal of Alloys and Compounds 506 (2010) 898–901

Contents lists available at ScienceDirect

Journal of Alloys and Compounds

journal homepage: www.elsevier.com/locate/jallcom

Intrinsic vacancies in cubic-zirconia bulk and surface

Pei Jun Shen[a,b,c,*], San Ping Jiang[c], Khuong Phuong Ong[b], Wei Zhong Ding[a], Pei-Lin Mao[d], Xiong Gang Lu[a], Chong He Li[a], Ping Wu[b]

[a] Department of Materials Science and Engineering, Shanghai University, China
[b] Computational Materials Science & Engineering Program, Institute of High Performance Computing, Singapore
[c] School of Mechanical & Aerospace Engineering, Nanyang Technological University, Singapore
[d] School of Chemical & Life Sciences, Nanyang Polytechnic, Singapore

ARTICLE INFO

Article history:
Received 7 May 2010
Received in revised form 13 July 2010
Accepted 13 July 2010
Available online 21 July 2010

PACS:
71.20.−b

Keywords:
Cubic-zirconia
Intrinsic vacancy
Formation energy

ABSTRACT

Formation of charged (neutral) vacancies of bulk (surface) cubic-ZrO_2 is calculated from density functional theory, and compared with available experiments. Relationships among vacancy formation energy, electron and element chemical potentials are established within a wide range of oxygen chemical potentials. The +2 (−2) oxygen (zirconium) vacancy is predicted stable near the valence (conduction) band edge of the bulk, and the neutral oxygen vacancy has the lowest formation energy on (1 0 0) O-terminated surface without exhibiting a defect state within the band gap. Therefore, manipulation of oxygen vacancy concentration becomes possible by optimizing growth surface and oxygen chemical potentials.

1. Introduction

Zirconia, ZrO2, is widely applied on catalyst [1], gas sensors [2], fuel cells [3–5], thermal barrier coating [6]. For instance, nanocrystalline ZrO_2–CeO_2 solid solutions showed excellent catalytic properties and exhibited high performance as anode in fuel cells because of the mixed ionic-electronic conduction in reducing atmosphere [5]. It is well known that defects play an important role for the properties of functional materials [7,8]. Previous studies focus mainly on the effects of oxygen vacancy to atomic structure, electronic properties, as well as oxygen ion mobility [9–17] in the stabilized (by doping) cubic-ZrO2, few models were also reported for defects in pure cubic- [10], monoclinic- [8] and tetragonal-ZrO2 [9,18–20]. A relationship among defect stability, electron chemical potential and element chemical potential is, however, not yet well established for pure ZrO2. In addition, the cubic-zirconia (stabilized either by dopant or nano-scale effects [21]) has the most abundant applications among the three polymorphs. In this work we systematically investigated the formation and electron band structures of intrinsic vacancies in pure bulk cubic-ZrO2 and its surface at a wide range of electron and element chemical potentials of interest to real applications. The resultant model could be used to provide guidance to the design of next generation ZrO2 based materials.

We first report a systematic study on the formation energy and pinning energy of intrinsic vacancies in cubic-zirconia under different electron and element chemical potentials, and then extend the calculations to surfaces of practical interest to catalyst research.

2. Calculation method

All calculations were performed using WIEN2k [22] software based on density functional theory (DFT) by utilizing the augmented plane wave (APW). The transition metal *d* state was calculated by the Augmented Plane Waves + local orbitals (APW + lo) basic set and others by the Linearized Augmented Plane Wave method (LAPW). The muffin tin radii (RMT) were 1.70 and 1.67 a.u. for Zr and O, respectively. Inside the atomic spheres, the partial waves were expanded up to $l_{max} = 10$. The number of plane waves was limited by the cut off $R_{mt} \times K_{max} = 7.00$. The calculation was iterated to self-consistency with the specified energy convergence criterion 10^{-5} Ry and charge convergence criterion 10^{-4} e. During relaxation, equilibrium positions of atoms are evaluated by a 'reverse-communication trust-region Quasi–Newton method' and the final forces on each atom is less than 1 mRy/a.u. The formation energies of vacancies are obtained by employing supercells with 81 atoms ($3 \times 3 \times 3$ supercell), in which $4 \times 4 \times 4$ *k*-points are selected for supercells calculations. Three types of low-index surfaces:

* Corresponding author at: Department of Materials Science and Engineering, Shanghai University, China. Tel.: +86 021 56338244; fax: +86 021 56338244.
E-mail address: shenpeijun@shu.edu.cn (P.J. Shen).

0925-8388/$ – see front matter © 2010 Elsevier B.V. All rights reserved.
doi:10.1016/j.jallcom.2010.07.108

Table 1
Formation energy of oxygen/zirconium vacancies (V_O^q/V_{Zr}^q) under 3 chemical conditions.

Vacancy	q (charge state)	ΔE (eV) (zirconium-rich)	ΔE (eV) (oxygen-rich)	ΔE (eV) (H_2/H_2O mixture)
V_O^q	0	0.50	6.63	3.93
	+1	−2.46	3.67	0.97
	+2	−5.26	0.87	−1.83
V_{Zr}^q	−4	16.00	3.75	9.15
	−3	15.77	3.52	8.92
	−2	15.74	3.49	8.89
	−1	15.85	3.60	9.00
	0	16.02	3.78	9.18

(0 0 1) O-termination, (0 1 1) surface, and (1 1 1) O-termination are investigated by using a periodic symmetric slab with 7 ZrO_2-laysers separated by 11.8504 Å vacuum region, in which $6 \times 6 \times 1$ k-points are selected for supercells calculations. The size of the surface model is (1×1) for (0 0 1) O-termination and (0 1 1) surface, while the size of (1 1 1) O-termination is (2×1) along the [1,−1,0] surface vector. We also test a few functionals by calculations of bulk ZrO_2 structure parameters, and finally in all calculations we select the GGA(WC) (Wu-Cohen06) which reproduces well the lattice constant (5.073 Å compare to the experiment value of 5.090 Å [23]). DFT calculations typically underestimate the band gap. We, therefore, assumed the offset of the calculated band structure to be restricted to the conduction band minimum (CBM) [23].

3. Results and discussion

For a stable ZrO_2 we have $\mu_{Zr} + 2\mu_O = \mu_{ZrO_2}$ and $\mu_{Zr}^{reference} + 2\mu_O^{reference} + \Delta H_{ZrO_2} = \mu_{ZrO_2}^{reference}$ [24], where μ_i is the chemical potential of component i; $\mu_i^{reference}$ is, respectively, the chemical potential at reference state (gas for oxygen and bulk for zirconia ($Fm3m$) and zirconium ($P63/mmc$)); ΔH_{ZrO_2} is the formation heat of ZrO_2 (calculated as −12.25 eV). To suspend the formation of bulk Zr and oxygen gas, $\mu_{Zr} \le \mu_{Zr}^{bulk}$ and $\mu_O \le \mu_O^{gas}$ have to be conserved, therefore ZrO_2 is stable in the range of $\mu_{ZrO_2}^{bulk} - \mu_{Zr}^{bulk} \le 2\mu_O \le \mu_{ZrO_2}^{bulk} - \mu_{Zr}^{bulk} - \Delta H_{ZrO_2}$ (or $1/2\Delta H_{ZrO_2} \le \Delta\mu_O \le 0$), where $\Delta\mu_O$ is the excess potential of oxygen. Besides the two extreme conditions we also consider the condition in equilibrium with H_2/H_2O mixtures (at $\Delta\mu_O$ equal to −2.7 eV at 0 K [25]) to understand the redox properties of zirconia under representative environment of applications.

The formation energy of a defect in a charge state q is given by [26]: $\Delta H_{D,q}(E_F, \mu) = (E_{D,q} - E_H) + \sum_\alpha n_\alpha \mu_\alpha + q(E_v + E_F)$, where $E_{D,q}$ and E_H are the total energy of the defected supercell in the charged state q and perfect supercell, respectively; The chemical potentials of the constituents are given by the second term, μ_α is the absolute value of the chemical potential of atom α, and n_α is the number of type α defect; The last term describes the energy change due to exchange of electrons and holes with carrier reservoirs, E_v represents the energy at the valence band maximum (VBM) of the defect free system, and E_F is the Fermi energy relative to the E_v. The calculated vacancy formation energy is shown in Table 1 and Fig. 1 as a function of Fermi levels at three studied oxygen chemical potentials.

Due to the large formation enthalpy of ZrO_2, the vacancy formation energies depend strongly on oxygen chemical potentials. The Fermi level is called a pinning energy, ε_{pin} [27] if the vacancy formation energy changes signs (from positive to negative) at this Fermi level. In Fig. 1(a), below the p-type pinning energy ε_{pin}^p, V_O^{2+} are spontaneously formed which act as hole killers to negate the introduced acceptors. Therefore, it is very difficult to realize p-type ZrO_2. Similarly, n-doping by donors will be neutralized by the spontaneous formation of V_{Zr}^{4-} who act as native electron killers above ε_{pin}^n (n-type pinning energy). V_O^{2+} is the most stable vacancy near VBM at all three chemical potentials, and its formation is exothermic and spontaneous in both oxygen-poor (Fig. 1(a)) and in equilibrium with H_2/H_2O (Fig. 1(c)). This is consistent with the experiment in which the lattice oxygen of zirconia could be removed (to form an oxygen vacancy) even at 300 °C thus additional oxygen atoms could participate in the bi-functional catalyst reactions [28]. At VBM, The formation of oxygen vacancy is spontaneous under oxygen-poor conditions, but not for the zirconium one even at a favored zirconium-poor condition. Therefore, a large population of V_{Zr} is unlikely in pure zirconia. This is also in line with experiments where V_{Zr} is observed at high temperature and along the grain boundary only [29].

In addition to the bulk, vacancy on surface is also of critical importance in practical applications. There are six types of low-index surfaces: (0 0 1) O-termination, (0 0 1) Zr-termination, nonpolar-(0 1 1) surface, nonpolar-(1 1 1) surface, (1 1 1) O-termination, and (1 1 1) Zr-termination. We believe the oxygen vacancy exposed on surface is the most important to the redox properties of zirconia, therefore three experimentally reported surfaces ((1 0 0), (1 1 0) and (1 1 1)) [30], (0 0 1) O-termination, (0 1 1) surface, and (1 1 1) O-termination, were investigated to understand the redox properties of zirconia. The respective calculated formation energy (at $\Theta_{def} = 1/2$ [18]) is lower

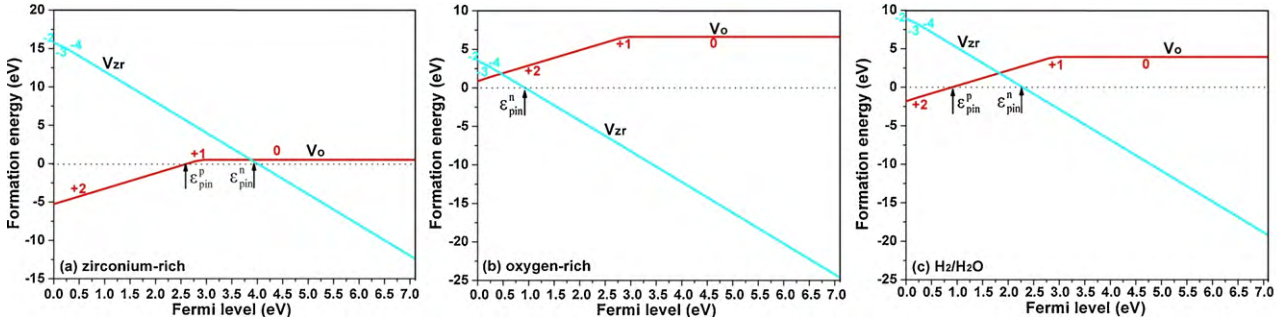

Fig. 1. Variation of vacancy formation energy with Fermi levels under 3 chemical conditions; (a) oxygen-poor, (b) oxygen-rich, and (c) in equilibrium with H_2/H_2O

Table 2
Structure relaxation of ions NN to the vacancies and corresponding relaxation energy (in bulk: '−'/'+' means inward/outward displacement to the vacancy).

Case		$V^0_{O,bulk}$	$V^{2+}_{O,bulk}$	$V^0_{Zr,bulk}$	$V^{2-}_{Zr,bulk}$	$V^0_{O,(1\,0\,0)}$	$V^0_{O,(1\,1\,0)}$	$V^0_{O,(1\,1\,1)}$
Relaxation size (Å)	NN_O	−0.084	−0.27	+0.154	+0.156	0.20	0.18	0.093
	NN_Zr	−0.020	+0.16	−0.052	−0.054	0.12	0.43	0.12

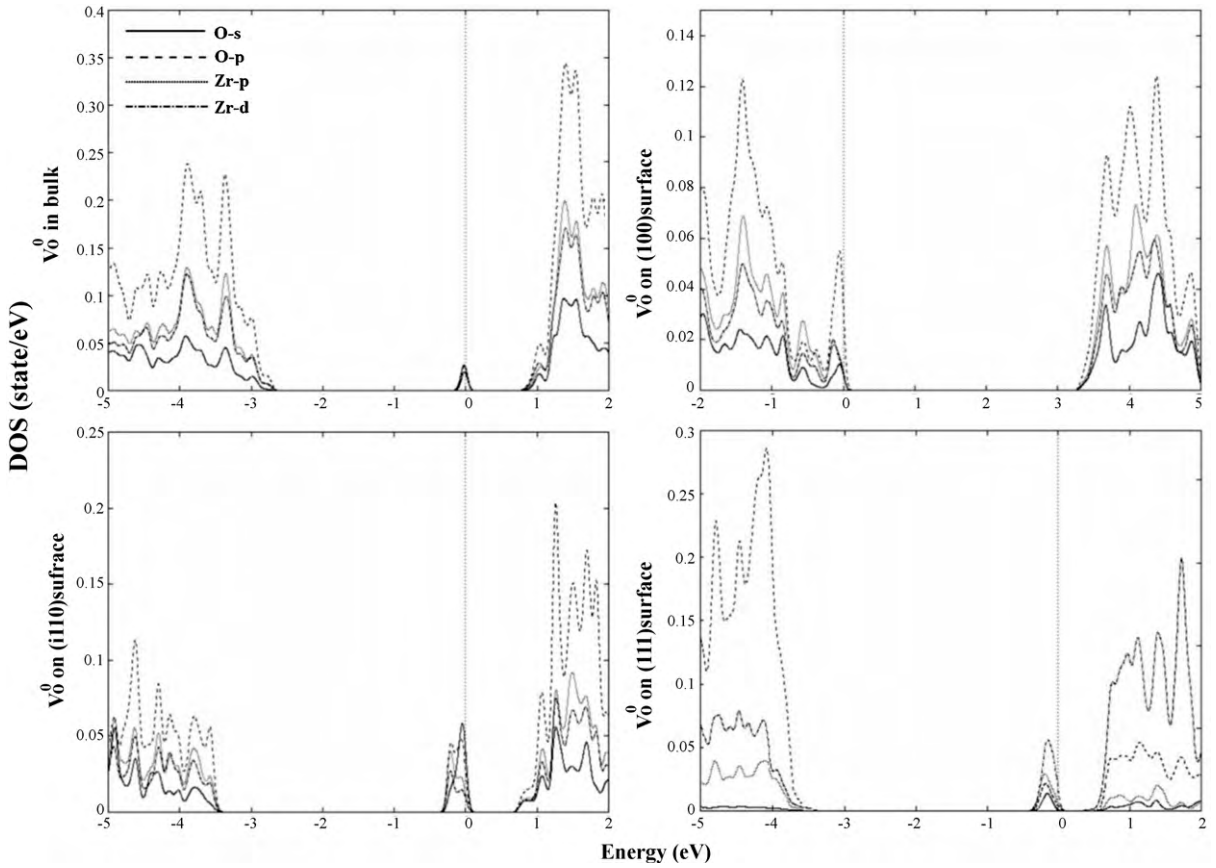

Fig. 2. Partial DOS of Zr- and O-ion neighboring vacancy.

than the one in the bulk at all considered oxygen chemical potentials; i.e. −1.48, 5.12 and 5.98 eV under O_2-rich condition (<6.63 eV in bulk), −7.18, −0.58 and 0.28 eV under Zr-rich condition (<0.50 eV in bulk), and −4.18, 2.42 and 3.28 eV under H_2/H_2O-mixture condition (<3.93 eV in bulk). Furthermore, the oxygen vacancy is predicted more stable on the polar (1 0 0) surface than on the nonpolar (1 1 1) and (1 1 0) ones. Consequently, the (1 0 0) surface would be reconstructed evidently through the removal of a large number of oxygen-ions, while such reconstruction is expected minimum on (1 1 1) surface whose vacancy formation energy is close to that in the bulk. Therefore it is possible to experimentally control the oxygen vacancy concentrations by applying different epitaxial growth surface and oxygen chemical potentials.

Details of the atomistic displacements surrounding the vacancy in the bulk and surfaces are shown in Table 2, in which NN_Zr (or NN_O) is the displacement (with reference to the perfect crystal) of the zirconium (or oxygen) atom occupying the nearest-neighbor position to the vacancy. Our calculations are inline with available reported data, for instance NN_Zr for V_O^{2+} and V_O^0, i.e. 0.16 and 0.02 Å, is respectively close to ~0.18 Å of YSZ [31] and 0.03–0.06 Å of [32]. In the bulk, ionization of V_{Zr}^0 to V_{Zr}^{2-} does not show evident changes in both NN_Zr (0.002 Å) and NN_O (0.002 Å) while the change is significant for V_O^0 to V_O^{2+}. Such different ionization behavior may contribute to the fact that the excess electrons is less strongly localized around V_{Zr}^{2-} than V_O^{2+}. To reveal the difference in structural relaxation among the bulk and the 3 surfaces, we compile their corresponding NN_O, NN_Zr data for V_O^0 only, where NN_O and NN_Zr reaches a maximum value (0.20 Å at (1 1 0) and 0.43 Å at (1 1 0)), respectively.

Similarly we discuss vacancy stability via the electronic structures of V_O^0 in the bulk and the three surfaces shown in Fig. 2. The O 2s and Zr 3p states are located far below the Fermi level in a perfect cell, however, with V_O^0 these states not only contribute significantly to the VBM and CBM but also strongly hybridized with the O 2p and Zr 4d states. In the bulk, V_O^0 would induce a defect state (color center) in the band gap, however, no electronic traps are presented in V_O^{2+} case because of the large inward relaxation (0.27 Å) of NN_O-ions that generates a Madelung field which prevents the formation of a deep state in the gap [10]. In addition, all zirconium vacancies do not induce any additional state in the band gap. For the surfaces, all V_O^0 except the one on (1 0 0) induce the defect state composed of Zr 3p/4d and O 2s/2p. The lack of this defect state for V_O^0 on the (1 0 0) surface may stabilize the vacancy accordingly.

4. Conclusions

In conclusion, formation of intrinsic vacancies in pure zirconia had been systematically investigated by first-principles calculations. It suggested that V_O^{2+} is the most stable vacancy near VBM in pure bulk zirconia under a wide range of oxygen chemical

potentials. At VBM, the formation of oxygen vacancy is spontaneous under oxygen-poor conditions, but not for the zirconium one even at a favored zirconium-poor condition. Vacancy formation energy of the oxygen (zirconium) increases (decreases) along with an increase in Fermi level. Stability of neutral oxygen vacancy not only depends on the dimension of the structure (higher on surface than in the bulk) but also the polarity nature of surface (higher on polar surface than the nonpolar ones). Additionally we demonstrate that the lack of a defect state in the band gap of the (1 0 0) surface may be the signature electronic structure for high vacancy stability. Therefore, manipulation of oxygen vacancy concentration becomes possible by applying the optimized growth surface and oxygen chemical potentials.

Acknowledgments

This work was conducted in the Institute of High Performance Computing (IHPC) of A*Star in Singapore. The authors are grateful to IHPC for the financial and computing facility support. Mr Peijun Shen is also partially supported financially by the National Foundation of Hi-tech Research and Development Program of China (National 863 Project of China, project No. 2006AA11A189), and the School of Mechanical and Aerospace Engineering in NANYANG Technological University (project No. T208A1216 (MoE AcRF T2)). Supports from all relevant agents are sincerely acknowledged.

References

[1] S.A. Steiner, T.F. Baumann, B.C. Bayer, R. Blume, M.A. Worsley, W.J. Moberly-Chan, E.L. Shaw, R. Schlogl, A.J. Hart, S. Hofmann, B.L. Wardle, J. Am. Chem. Soc. 131 (2009) 12144.
[2] P. Shuk, E. Bailey, U. Guth, Mod. Sens. Technol. 90 (2008) 174.
[3] J. Ding, J. Liu, W.M. Guo, J. Alloys Compd. 489 (2009) 286.
[4] M. Liu, C. He, J. Wang, W. Wang, Z. Wang, J. Alloys Compd. 502 (2010) 319.
[5] D.G. Lamas, M.F. Bianchetti, M.D. Cabezas, N.E. Walsoe de Reca, J. Alloys Compd. 495 (2010) 548.
[6] X. Song, M. Xie, X. Hao, F. Jia, S. An, J. Alloys Compd. 497 (2010) L5.
[7] J. Zhu, S. Alberstsma, J.G. van Ommen, L. Lefferts, J. Phys. Chem. B 109 (2005) 9550.
[8] A.S. Foster, V.B. Sulimov, F. Lopez Gejo, A.L. Schluger, R.M. Nieminen, Phys. Rev. B 64 (2001) 224108.
[9] A. Eichler, Phys. Rev. B 64 (2001) 174103.
[10] G. Stapper, M. Bernasconi, N. Nicoloso, M. Parrinello, Phys. Rev. B 59 (1999) 797.
[11] R. Devanathan, W.J. Weber, S.C. Singhal, J.D. Gale, Solid State Ionics 177 (2006) 1251.
[12] A. Bogicevic, C. Wolverton, Europhys. Lett. 56 (2001) 393.
[13] A. Bogicevic, C. Wolverton, Phys. Rev. B 67 (2003) 024106.
[14] K.S. Chang, K.L. Tung, Chem. Phys. Chem. 10 (2009) 1998.
[15] T. Viefhaus, T. Bolse, K. Muller, Solid State Ionics 177 (2006) 3063.
[16] M. Kilo, C. Argirusis, G. Borchardt, R.A. Jackson, Phys. Chem. Chem. Phys. 5 (2003) 2219.
[17] M. Kilo, R.A. Jackson, G. Borchardt, Phil. Mag. 83 (2003) 3309.
[18] M.V. Ganduglia-Pirovano, A. Hofmann, J. Sauer, Surf. Sci. Rep. 62 (2007) 219.
[19] A.A. Safonov, A.A. Bagatur'yants, A.A. Korkin, Microelectron. Eng. 69 (2003) 629.
[20] Alex Zunger, NCPV and Solar Program Review Meeting, 2003.
[21] M. Forker, P. de la Presa, W. Hoffbauer, S. Schlabach, M. Bruns, D.V. Szabo, Phys. Rev. B 77 (2008) 054108.
[22] K. Schwarz, P. Blaha, Comput. Mater. Sci. 28 (2003) 259.
[23] Paul Erharta, Karsten Albe, J. Appl. Phys. 102 (2007) 084111.
[24] M.C. Munoz, S. Gallego, J.I. Beltran, J. Cerda, Surf. Sci. Rep. 61 (2006) 303.
[25] X.G. Wang, A. Chaka, M. Scheffler, Phys. Rev. Lett. 84 (2000) 3650.
[26] C. Persson, Y.J. Zhao, S. Lany, Alex Zunger, Phys. Rev. B 72 (2005) 035211.
[27] S.B. Zhang, S.H. Wei, A. Zunger, Phys. Rev. Lett. 84 (2000) 1232.
[28] K.G. Azzam, I.V. Babich, K. Seshan, L. Lefferts, J. Catal. 251 (2007) 153.
[29] U. Chon, S.K. Lee, H.J. Kim, RIST 11 (1997) 282.
[30] C. Morterra, G. Cerrato, L. Ferroni, A. Negro, L. Montanaro, Appl. Surf. Sci. 65–66 (1993) 257.
[31] D. Steele, B.E.F. Fender, J. Phys. C 7 (1974) 1.
[32] D.M. Ramo, P.V. Sushko, J.L. Gavartin, A.L. Shluger, Phys. Rev. B 78 (2008) 235432.